

Cite this: *Dalton Trans.*, 2016, **45**, 17030

The half-sandwich 18- and 16-electron arene ruthenium iminophosphonamide complexes†

Tat'yana A. Peganova,^a Iana S. Sinopalnikova,^a Alexander S. Peregudov,^a Ivan V. Fedyanin,^a Albert Demonceau,^b Nikolai A. Ustynyuk^a and Alexander M. Kalsin^{*a}

Novel half-sandwich 18e and 16e arene ruthenium iminophosphonamide complexes $[(\eta^6\text{-C}_6\text{Me}_6)\text{RuCl}((\text{R}'\text{N})_2\text{PR}_2)]$ (**3a–c**) and $[(\eta^6\text{-C}_6\text{Me}_6)\text{Ru}((\text{R}'\text{N})_2\text{PR}_2)]^+(X^-)$ (**4a–c**) (**a**, R = Ph, R' = *p*-Tol; **b**, R = Et, R' = *p*-Tol; **c**, R = Ph, R' = Me. X = BF₄, PF₆ or BAR^F₄) were synthesized. The elongated Ru–Cl bond in the 18e complexes is shown to dissociate even in apolar solvents to form the corresponding 16e cations, which can be readily isolated as salts with non-coordinating anions. The coordinatively unsaturated 16e complexes are stable species due to efficient π -electron donation from the nitrogen atoms of the zwitterionic NPN-ligand. The ruthenium iminophosphonamides are moderately active in the ROMP polymerization of norbornene; the 16e complexes **4a,b** yield high molecular weight polymers ($M_n \sim 300 \times 10^3$) with a narrow distribution $M_w/M_n \sim 1.6$, while the 18e complexes **3a,b** give polymers of lower molecular weight ($M_n < 50 \times 10^3$) with a wider polydispersity index $M_w/M_n \sim 2.5$.

Received 11th August 2016,
Accepted 16th September 2016

DOI: 10.1039/c6dt03202h

www.rsc.org/dalton

Introduction

Among transition metal complexes with $\kappa^2\text{-N,N}$ -heteroallylic ligands, the iminophosphonamides bearing a coordinated $\text{R}_2\text{P}(\text{NR}')_2^-$ anion (NPN) are studied fragmentarily; there have been less than a hundred of molecular structures of NPN complexes established to date, that is in sharp contrast to more than a thousand of transition metal amidinate structures, according to the Cambridge Structural Database (CSD). The IV group metals,^{1–6} chromium,^{7–10} nickel^{11–15} and copper^{16–22} iminophosphonamides are the most studied, which is due to their catalytic application in cyclopropanation,^{16,21,23} olefin oligomerization^{7–9} and polymerization.^{2,6,12,15,24,25} A few platinum metal group iminophosphonamides have been reported for palladium²⁴ and ruthenium²⁶ before 2009, when we started systematic studies of these complexes. We have demonstrated experimentally from the precision X-ray data by determining the deformational electron density for the palladium complex $[\text{Pd}\{(p\text{-}^i\text{PrC}_6\text{H}_4\text{N})_2\text{PPh}_2\}]$ that the iminophosphonamide

ligand is zwitterionic $\text{N}^-\text{P}^+\text{-N}^-$ having single P–N bonds and bearing full negative charges at the nitrogen atoms.²⁷ This result shows a big difference between the electronic properties of iminophosphonamide and amidinate complexes, which previously have been considered as having a similar heteroallylic delocalized π -electronic system. The HOMO orbital of the zwitterionic NPN ligand may have either C_{2v} or C_s symmetry,²⁸ of which the latter can efficiently donate the π -electron density from the nitrogen atoms to the d_{xz} -orbital of the metal located in the plane of the ligand, similarly to the β -diketiminate complexes (Chart 1A and B). In contrast, the C_{2v} symmetry of the HOMO orbital in the amidinate ligand allows π -donation only by lateral coordination of the amidinate ligand resulting in a strong folding of the four-membered metallacycle (Chart 1C).

Indeed, the electron deficient ruthenium complexes can be stabilized by intramolecular π -coordination of the amidinate ligand, which leads to strong puckering of the Ru–N–C–N metallacycle in the 16e complexes $[(\text{Cp}^*)\text{Ru}\{(\text{tBuN})_2\text{C}(\text{Mes})\}]$ ²⁹ and $[(\text{C}_6\text{Me}_6)\text{Ru}\{(\text{tPrN})_2\text{CMe}\}]$ ³⁰ to 39.9° and 31.5°, respectively. The lateral coordination of the amidinate ligand stabilizes these 16e complexes inefficiently since it weakens the M–N σ -bonds; such species are very reactive and can readily coordinate 2e donors^{30–32} or other organometallic moieties to form dinuclear μ^2 -amidinate complexes.³³ At the same time, the solely reported ruthenium iminophosphonamide, the stable 16e $[(p\text{-cymene})\text{Ru}\{(\text{tPrN})_2\text{PPh}(\text{NH}^i\text{Pr})\}](\text{BPh}_4)$, did not react either with $[\text{Et}_3\text{NH}]\text{Cl}$, $[\text{PPh}_4]\text{Cl}$ or with triphenylphosphine and triphenyl phosphite to form 18e adducts; only carbon monoxide or cyanide could coordinate, however the corres-

^aA.N. Nesmeyanov Institute of Organoelement Compounds, Russian Academy of Sciences, 28 Vavilov str., 119991 Moscow, Russia. E-mail: kalsin@ineos.ac.ru

^bLaboratory of Macromolecular Chemistry and Organic Catalysis, Department of Chemistry, University of Liège, Sart-Tilman (B6a), 4000 Liège, Belgium

† Electronic supplementary information (ESI) available: Variable-temperature ¹H NMR of **3b** in toluene and the ΔG^\ddagger calculations for the exchange of Et_a and Et_b in **3b** in CD_2Cl_2 . CCDC 1475876–1475879, 1494098 and 1494099. For ESI and crystallographic data in CIF or other electronic format see DOI: 10.1039/c6dt03202h



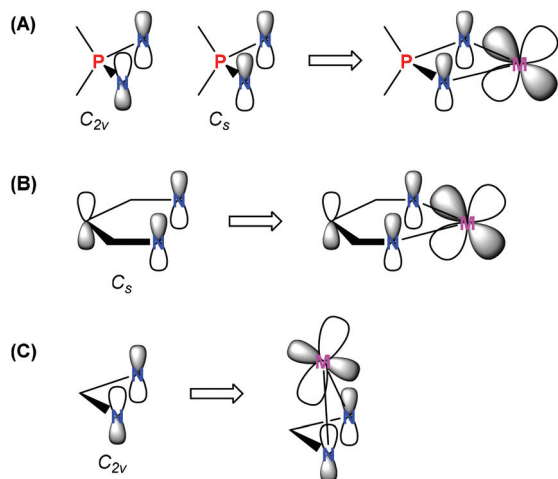


Chart 1 Schematic drawing of the HOMO orbitals of (A) iminophosphonamide, (B) β -diketiminato, and (C) amidinate ligands (on the left) and possible π -bonding with the d-orbital of the metal (on the right).

ponding $18e^-$ complexes were not isolated.²⁶ For this complex the authors proposed a possibility of pseudo π -allyl donation to ruthenium based on a slight puckering of the Ru–N–P–N plane by 13.9° . Since that time the chemistry of ruthenium iminophosphonamides has not progressed, although two structures of $18e^-$ $[(p\text{-cymene})\text{RuBr}\{(p\text{-TolN})_2\text{PMe}(p\text{-TolNH})\}]$ and $17e^-$ $[(\text{Cp}^*)\text{RuCl}\{(p\text{-TolN})_2\text{PMe}(p\text{-TolNH})\}]$ complexes were deposited in CSD in 2004–2005 but their synthesis and properties were not published.

Recently, an interesting arene ruthenium bis(phosphinimino)methanide complex $[(p\text{-cymene})\text{Ru}(\text{L})\text{Cl}]$ ($\text{L} = \text{PhN}(\text{PPh}_2)\text{CH}(\text{PPh}_2)\text{NPh}$) has been shown to exist as a cationic $18e^-$ complex with a tridentate $\kappa^3\text{-C,N,N}$ ligand L .³⁴ Although this ligand closely relates to iminophosphonamides, the stabilization of the $16e^-$ species occurs by intramolecular coordination of the methanide group but not by the unpaired electron density from the nitrogen atoms. Indeed the displacement of the methanide group by Cl^- or MeCN is highly unfavorable with the ΔG_{298}° calculated for the latter reaction to be $+19 \text{ kcal mol}^{-1}$. This complex fails to react with CO under ambient conditions, which has also been attributed to the high nucleophilicity of the methanide group and the weak π -basicity of the ruthenium center.³⁵

Here we report the synthesis of a series of new $18e^-$ and $16e^-$ half-sandwich arene ruthenium complexes with various iminophosphonamide ligands distinguished by the electronic properties of their N - and P -substituents, their physico-chemical and structural data in comparison to other $\kappa^2\text{-N,N}$ -heteroallylic arene ruthenium complexes, and preliminary catalytic data for the ring-opening metathesis polymerization (ROMP) of norbornene.

Results and discussion

Synthesis and characterization of the complexes 3–4

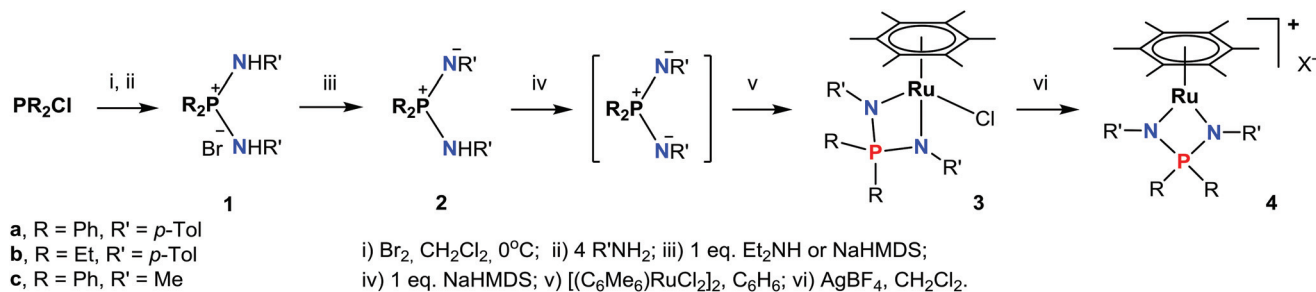
The synthesis of arene ruthenium NPN-complexes (3–4) from the diamminophosphonium salts **1a–c** is summarized in Scheme 1.

The diamminophosphonium salts $[\text{R}_2\text{P}(\text{NHR}')_2]\text{Br}$ (**1a–c**) were prepared in high yields, according to the earlier developed procedure.³⁶ The salts **1a–c** can be monodeprotonated with strong bases like NaHMDS or $n\text{-BuLi}$ to give the corresponding iminophosphonamines **2a–c**, while the more acidic **1a** is deprotonated easily with an equimolar amount of Et_2NH to yield **2a** quantitatively. At the same time, NaHMDS is preferred for the synthesis of **2b** and **2c**; when $n\text{-BuLi}$ is employed, the isolation of these iminophosphonamines is very laborious due to their complexation with lithium salts. The new compounds **1b** and **2a,b** were fully characterized spectroscopically and by elemental analysis, while we were not able to obtain satisfactory elemental analysis for **2c** due to its high moisture sensitivity. In ^{31}P NMR the phosphorus signals of **2a–c** are shifted by 27–32 ppm to less positive values compared to those of **1a–c**. In ^1H NMR, the NH hydrogen of **1a** (δ 9.26) is more acidic than the NH groups of **1b** (δ 8.77) and **1c** (δ 6.61) thus reflecting the electron-releasing effect of the N - and P -substituents on the electron density at the nitrogen atoms. Expectedly, the basic NH resonances of the iminophosphonamines **2a** (δ 5.55) and **2b** (δ 3.85) are shifted to less positive values. The signals from chemically inequivalent substituents at the nitrogen atoms in iminophosphonamines **2a,b** are averaged tentatively due to intermolecular N–H...N proton exchange;³⁷ perhaps such exchange is responsible for not observing the NH signal for **2c**.

Further deprotonation of **2a–c** with 1 equiv. of NaHMDS results in the formation of sodium iminophosphonamides $\text{Na}[\text{R}_2\text{P}(\text{NR}')_2]$, as indicated by the new signals in ^{31}P NMR at more positive values δ 7.0 ($\text{R} = \text{Ph}$, $\text{R}' = p\text{-Tol}$), δ 29.0 ($\text{R} = \text{Et}$, $\text{R}' = p\text{-Tol}$) and δ 28.5 ($\text{R} = \text{Ph}$, $\text{R}' = \text{Me}$) with respect to the corresponding iminophosphonamines **2a–c**;^{14,27,38} however they were not isolated due to extremely high moisture sensitivity. The iminophosphonamides $\text{Na}[\text{R}_2\text{P}(\text{NR}')_2]$ generated *in situ* react with the dimeric ruthenium complex $[(\eta^6\text{-C}_6\text{Me}_6)\text{RuCl}_2]_2$ to give the corresponding $18e^-$ arene ruthenium(II) complexes **3a–c** with the chelating bidentate NPN-ligand in moderate-to-high isolated yields (62–86%). The chloride ligand in **3a–c** was easily replaced with the non-coordinating anions (PF_6^- , BF_4^- , BAR_4^{F}) by treating them with the corresponding silver or sodium salts in dichloromethane to afford the new $16e^-$ cationic complexes $[(\eta^6\text{-C}_6\text{Me}_6)\text{Ru}\{(p\text{-TolN})_2\text{PPh}_2\}](\text{PF}_6)$ (**4a**), $[(\eta^6\text{-C}_6\text{Me}_6)\text{Ru}\{(p\text{-TolN})_2\text{PEt}_2\}](\text{BF}_4)$ (**4b**) and $[(\eta^6\text{-C}_6\text{Me}_6)\text{Ru}\{(\text{MeN})_2\text{PPh}_2\}](\text{BAR}_4^{\text{F}})$ (**4c**) in nearly quantitative yields as deep-violet solids. All the complexes obtained were fully characterized by NMR spectroscopy and elemental analysis and their molecular structures were confirmed by single crystal X-ray diffraction studies. The selected structural parameters of **3a–c** and **4a–c** are given in Table 1 and their projections are shown in Fig. 1–6.

The $18e^-$ complexes **3a–c** exhibit a three-legged piano stool geometry with a pseudo-octahedral configuration of the ligands around the ruthenium atom. The Ru– C_6Me_6 (centroid) distance is in the range of 1.675(3)–1.662(4) Å, which is typical of neutral half-sandwich arene ruthenium complexes. Similarly to the β -diketiminato arene ruthenium complex,³⁹ in both **3a,b** the C–C bond lengths in the η^6 -coordinated arene noticeably alternate: the bonds C(2)–C(3), C(4)–C(5), and C(1)–C(6), which are





Scheme 1 Synthesis of complexes 3–4.

Table 1 Selected geometrical parameters of complexes 3a–c and 4a–c: the distances (Å), angles and dihedrals (°)

	3a	3b	3c	4a	4b	4c
Ru...C ₆ Me ₆ (centroid)	1.675(3)	1.666(2)	1.662(4)	1.662(2)	1.675(1)	1.652(4)
Ru–C(arene)	2.175–2.233(3)	2.171–2.217(2)	2.159–2.218(4)	2.149–2.252(2)	2.143–2.275(1)	2.142–2.208(4)
Ru–N ₁	2.137(2)	2.151(2)	2.137(4)	2.017(2)	2.0119(11)	2.011(4)
Ru–N ₂	2.171(2)	2.161(2)	2.159(4)	2.036(2)	2.0733(10)	2.020(3)
P–N ₁	1.600(2)	1.603(2)	1.605(4)	1.623(2)	1.6352(10)	1.615(4)
P–N ₂	1.613(3)	1.615(2)	1.602(4)	1.624(2)	1.6233(10)	1.619(4)
Ru–Cl	2.438(3)	2.437(2)	2.445(4)			
N ₁ –Ru–N ₂	68.08(9)	68.08(7)	69.39(14)	72.33(9)	72.17(4)	72.93(14)
N ₁ –P–N ₂	97.30(12)	97.22(10)	99.36(19)	94.87(12)	95.22(5)	95.57(18)
Ru–N ₁ –P	97.98(11)	96.81(9)	95.94(18)	96.54(11)	94.82(5)	95.50(17)
Ru–N ₂ –P	96.25(11)	96.07(9)	95.15(17)	95.81(11)	97.56(5)	95.01(17)
Ru–N(1)–N(2)–P	173.69(15)	166.25(12)	175.9(3)	173.23(15)	175.02(6)	169.7(2)
C ₆ Me ₆ (centroid)–Ru–P	142.2	148.7	148.2	176.0	174.1	175.6
Ru–C(1)–C(4)/Ru–N(1)–N(2)				6.3	5.7	26.1
∑(N ₁) ^a	359.2(5)	354.5(4)	357.6(8)	360.0(5)	359.8(2)	359.0(8)
∑(N ₂) ^a	358.6(5)	354.6(4)	344.4(8)	354.9(5)	360.0(2)	356.9(8)

^a The sum of bond angles at the corresponding nitrogen atom.

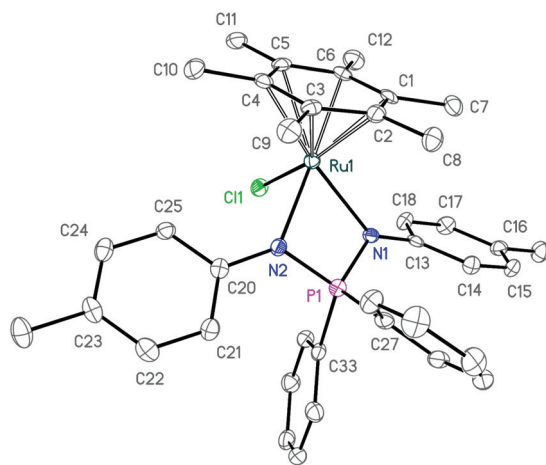


Fig. 1 ORTEP diagram of complex 3a. Ellipsoids are shown at 50% probability, hydrogen atoms are omitted for clarity.

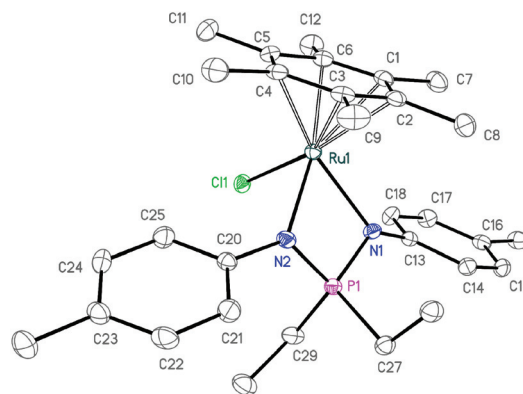


Fig. 2 ORTEP diagram of complex 3b. Ellipsoids are shown at 50% probability, hydrogen atoms are omitted for clarity.

trans to the N(1), N(2) and Cl(1), are shorter (1.412–1.421 Å for 3a and 1.417–1.423 Å for 3b) than the bonds C(1)–C(2), C(3)–C(4), and C(5)–C(6) (1.436–1.442 Å for 3a and 1.442–1.447 Å for 3b). In contrast to this, in 3c the coordinated arene gives a nearly eclipsed conformation with the chloride and the NPN-

ligands; only N(1) significantly deviates from that (the torsion angle N(1)–Ru–C₆Me₆(centroid)–C(1) is 18.5°), which results in shortening of the C(4)–C(5) bond *trans* to N(1) (1.417 Å), while the other C–C bonds are slightly longer (1.428–1.441 Å).

In iminophosphonamide complexes 3a–c the Ru–N bonds (2.137–2.171 Å) and the Ru–Cl bonds (2.437–2.445 Å) are considerably longer than those in analogous 18e arene ruthenium



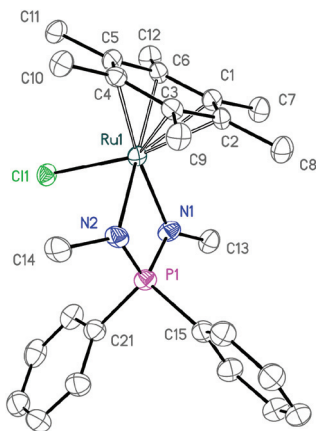


Fig. 3 ORTEP diagram of complex **3c**. Ellipsoids are shown at 50% probability, hydrogen atoms are omitted for clarity.

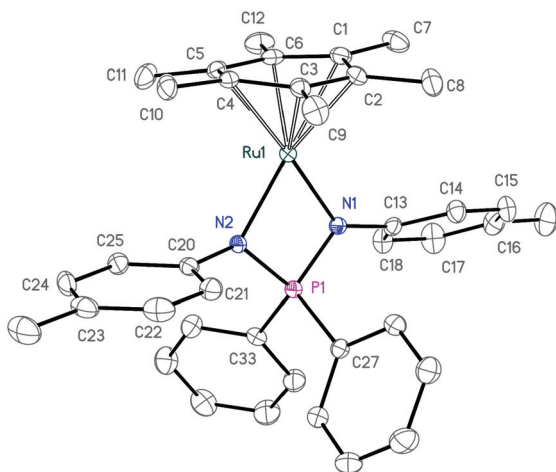


Fig. 4 ORTEP diagram of cation **4a**. Ellipsoids are shown at 50% probability, hydrogen atoms and the anion are omitted for clarity.

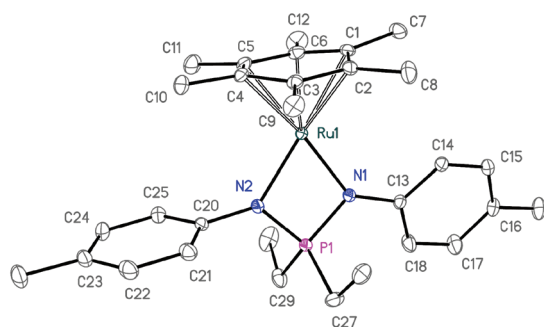


Fig. 5 ORTEP diagram of cation **4b**. Ellipsoids are shown at 50% probability, hydrogens atoms and the anion are omitted for clarity.

amidinate (2.078–2.139 Å and 2.400–2.434 Å, respectively)^{40–44} or triazenide (2.104–2.133 Å and 2.386–2.397 Å)⁴⁵ complexes, perhaps due to the high negative charge located at the nitrogen atoms of the zwitterionic NPN-ligand. Indeed, the Ru–Cl

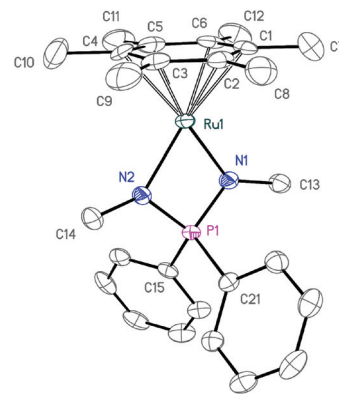


Fig. 6 ORTEP diagram of the cation **4c**. Ellipsoids are shown at 50% probability, hydrogen atoms and the anion are omitted for clarity.

bond is elongated in arene ruthenium complexes with highly efficient σ,π -donating β -diketiminate (2.461–2.521 Å)^{39,46,47} or dianionic bis(imidazolin-2-iminate) (2.4853(4) Å) ligands,⁴⁸ up to full dissociation in the latter example.

The chlorine atom has intramolecular close CH...Cl contacts with one *ortho*-hydrogen (H18A) of the *N*-tolyl substituents. The H18A...Cl distances in **3a** (2.762 Å) and **3b** (2.813 Å) fall below the sum of the van der Waals radii of 2.95 Å (ref. 49 and 50) and the corresponding angles Cl...H–C of 140.4° (**3a**) and 140.8° (**3b**) are typical of such a type of non-directed interaction. The chlorine atom is almost coplanar to the plane of the tolyl ring involved in the H...Cl contact and the corresponding torsion angle Cl–H(18A)–C(18)–C(13) is 7.6° and 8.4° for **3a** and **3b**, respectively. A few other intra- and intermolecular close contacts H...Cl are observed in **3a,b** with the hydrogens of the C₆Me₆ ligand (the Cl...H11C, Cl...H11B distances are 2.772, 2.749 Å in **3a** and the Cl...H11C, Cl...H8A are 2.899, 2.871 Å in **3b**) and of the *P*-substituent (the Cl...H34A is 2.868 Å in **3a** and the Cl...H29A is 2.812 Å in **3b**). Similar intra- and intermolecular close contacts can be seen in **3c** between the chlorine atom and the hydrogen atoms of the methyl group at N(2) (Cl...H14B is 2.872 Å) and C₆Me₆ (Cl...H10C is 2.840 Å), respectively.

The chelate angle N(1)–Ru–N(2) in **3a–c** (68.1–69.4°) is significantly larger than that in the analogous 18e[−] ruthenium amidinate complexes (61–62°),^{40–43,51} since the P–N bonds are longer than the corresponding C–N bonds in the amidinates. It is worth noting that the torsion angle Ru–N(1)–N(2)–P is close to 180° showing small puckering of the Ru–N(1)–P–N(2) metallacycle from the planarity (6.3° for **3a**, 13.7° for **3b** and 4.1° for **3c**). The pyramidalization of the nitrogen atoms is rather small in **3a,b**, while it is strong for one of the nitrogens in **3c**, for which the sum of the angles at the N(2) atom $\sum(\text{N})$ is 344.4°. Recently, a much wider range of puckering angles (up to 23.4°) and relatively strong pyramidalization of one of the nitrogen atoms (348–351°) were observed in the square-planar palladium iminophosphoramidate complexes, presumably as a result of steric repulsion between the *N*-cumyl substituents of the NPN- and co-ligands.²⁷ However this seems to be not the



case of **3c** bearing sterically small *N*-methyl groups; more probably the pyramidalization of N(2) is due to the high unpaired electron density located fully at the nitrogen atom and being not able to delocalize on any other electron system like aromatic *N*-tolyl groups in **3a,b**.

The 16 \bar{e} cationic complexes **4a–c** expectedly exhibit a two-legged piano-stool geometry with the chelating NPN-ligand positioned nearly perpendicular to the C₆Me₆ ring; the C₆Me₆ (centroid)–Ru–P angle is 174–176°. The Ru–C₆Me₆ (centroid) distance is 1.652–1.675 Å and is similar to that in **3a–c**. The Ru–N bond lengths in **4a–c** (2.011–2.073 Å) are close to those in [(*p*-cymene)Ru{(iPrN)₂PPh(NH⁺iPr)}](BPh₄) (**5**) (2.011, 2.017 Å)²⁶ and are significantly shorter than in **3a–c** due to stronger binding with the positively charged ruthenium atom. Slightly shorter Ru–N distances were reported for 16 \bar{e} cationic β -diketiminates (1.994–1.997 Å)³⁹ and bis(imidazolin-2-iminates) (1.977–2.003 Å),⁴⁸ while in the analogous ruthenium amidinate complexes these bonds are longer (2.058–2.065 Å),^{30,32} showing the intermediate donating ability of the NPN-ligand. The C₆Me₆ ring is not planar but is significantly distorted towards the boat conformation making four Ru–C(arene) bonds shorter (2.149–2.178(2) Å in **4a** and 2.143–2.199(1) Å in **4b**) and two bonds, namely Ru–C(1) and Ru–C(4) (2.238(2), 2.252(2) Å for **4a** and 2.228(1), 2.275(1) Å for **4b**), longer. Unlike in the 18 \bar{e} complexes **3a,b**, the C–C bonds in C₆Me₆ in **4a,b** do not alternate, instead the bonds C(2)–C(3) and C(5)–C(6) (1.440–1.444 Å) are slightly longer than the other four C–C bonds (1.418–1.428 Å) as a result of the stronger bonding of these carbons with the ruthenium atom. Importantly, in **4a,b** the longer Ru–C(1) and Ru–C(4) bonds are always *trans* to the Ru–N bonds (the dihedral angle between the planes Ru–C(1)–C(4) and Ru–N(1)–N(2) is 5.7–6.3°) with the longest Ru–C(4) bond *trans* to the shortest Ru–N(2) bond. A similar distortion of the coordinated arene planarity and the Ru–C(arene) bond distribution was earlier observed for **5**²⁶ and dicationic arene ruthenium complexes with the bis(imidazolin-2-imine) ligand.⁴⁸ It should be noted that in **4c** the arene and the NPN-ligand are in a staggered conformation (the dihedral angle between the planes Ru–C(2)–C(5) and Ru–N(1)–N(2) is 86.1°), which leads to slight shortening of the Ru–C(2) and Ru–C(5) (2.142(4), 2.163(4) Å) compared to the other four Ru–C(arene) bonds (2.177–2.208 Å) resulting in a flipped boat conformation of the arene.

The chelate angle N(1)–Ru–N(2) in **4a–c** (72.1–72.9°) is almost equal to that in **5** (71.8°)²⁶ and larger by *ca.* 4° than in **3a–c**. The pyramidalization of the nitrogen atoms ($\sum(N)$ is 355–360°) and the puckering of the plane Ru(1)N(1)P(1)N(2) (5.0–10.3°) are small. This is in sharp contrast to the strong puckering (31.4°) of the chelate metallacycle M–N–C–N in the analogous amidinate 16 \bar{e} arene ruthenium complex [(η^6 -C₆Me₆)Ru{(N⁺iPr)₂CMe}](PF₆), required for additional stabilization of the coordinatively unsaturated species by a π -heteroallyl system.³⁰

The structural peculiarities of the coordinated arene, the flattened RuNPN metallacycle and the short Ru–N bonds in **4a–c** are indicative of the strong σ,π -bonding of the iminopho-

sphoramidate ligand²⁶ *via* nitrogen atoms, similarly to β -diketiminates and bis(imidazolin-2-iminates), and in contrast to allylic π -stabilization in metal amidinates. The elongated Ru–Cl bonds in **3a–c** and the pyramidalization of the nitrogen atom in the most electron-rich **3c** are also in agreement with the zwitterionic structure of the NPN ligand bearing enhanced negative charges at the nitrogen atoms.

In the ³¹P NMR spectra of **3a,b** the phosphorus resonance (δ 43.9 for **3a** and δ 72.4 for **3b**) is shifted by *ca.* 47–49 ppm to more positive values compared to the precursors **2a** and **2b**. Interestingly, in the ¹H NMR spectra of **3a** and **3b** in CDCl₃ the two chemically inequivalent substituents at the phosphorus atom give only one set of signals for phenyl and ethyl groups, respectively. However, in the ¹H NMR spectra recorded in apolar C₆D₆, the *P*-substituents of **3a** and **3b** give rise to two sets of the corresponding resonances. Similarly, in the ¹³C NMR spectra of **3a** and **3b** in CDCl₃ the resonances for only one type of phenyl and ethyl groups are observed. It is noteworthy that in ¹³C NMR the characteristic doublets for *ipso*-carbons of phenyls are not found, perhaps due to their strong broadening. Apparently, in polar solvents fast exchange between the two *P*-substituents takes place. Indeed, heating a solution of **3a** and **3b** in apolar toluene-*d*₈ (*T* = 273–353 K) leads to broadening of the inequivalent phenyl and ethyl resonances, respectively for **3a** and **3b**, in ¹H NMR, though their coalescence is not achieved (see the ESI†). In a more polar CD₂Cl₂ solution of **3b** at 298 K the signals for only one ethyl substituent are observed, while decreasing the temperature to 193 K gives two separate resonances of methyl groups (Fig. 7). At the coalescence temperature of *T*_c = 238 K in dichloromethane, the estimated exchange rate constant is 1370 s^{−1} and the free energy of activation ΔG^\ddagger calculated from the Eyring equation is about 10.4 kcal mol^{−1}.⁵²

The exchange between the *P*-substituents R_a and R_b seems to proceed *via* a C_{2v}-symmetric intermediate or a transition state with two equivalent R groups, tentatively the cationic complex [(η^6 -C₆Me₆)Ru{R₂P(N-*p*-Tol)₂}]⁺Cl[−] (*vide infra*), formed from **3a,b** by dissociation of the chloride anion (Scheme 2).

Although the dissociation of the chloride anion in 18 \bar{e} complexes **3a,b** is facile in CDCl₃ or CD₂Cl₂, the equilibrium concentration of the dissociated 16 \bar{e} form is negligible, as far as their signals in ³¹P NMR in CDCl₃ (δ 43.9 for **3a**, δ 72.4 for **3b**) and C₆D₆ (δ 43.3 for **3a**, δ 71.1 for **3b**) remain virtually unchanged. The phosphorus resonance of the 16 \bar{e} cationic complexes **4a** (δ 71.9) and **4b** (δ 102.3) is strongly shifted by ~30 ppm to more positive values compared to the neutral complexes **3a,b**. In the ¹H and ¹³C NMR spectra of **4a,b** in CD₂Cl₂ the *P*-substituents are chemically equivalent, independent of the temperature (193–298 K) as it is expected for C_{2v}-symmetric complexes.

In apolar C₆D₆ complex **3c** also gives rise to two inequivalent phenyl groups in the ¹H and ¹³C NMR spectra, which is consistent with the non-dissociated 18 \bar{e} chloride complex, though the signals are broadened. Whereas in more polar CDCl₃ complex **3c** has violet color and its ³¹P resonance (δ 76.9) is strongly shifted to more positive values than in C₆D₆ (δ 59.8) and becomes close to the signal of the cationic



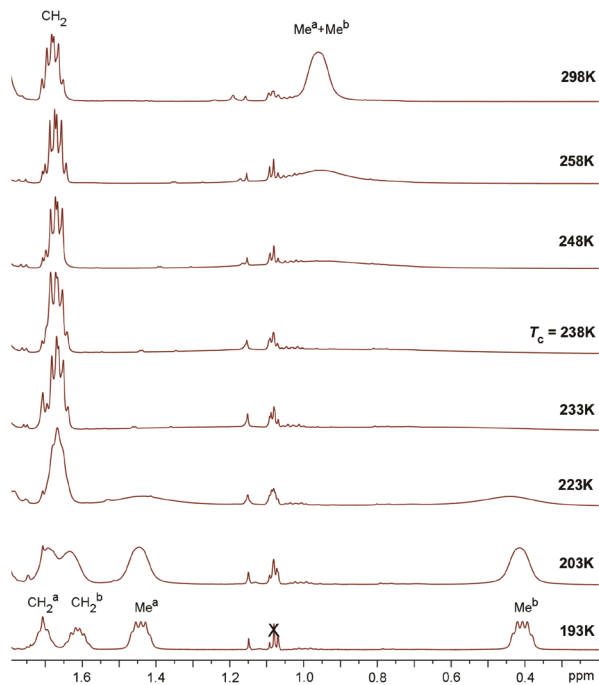
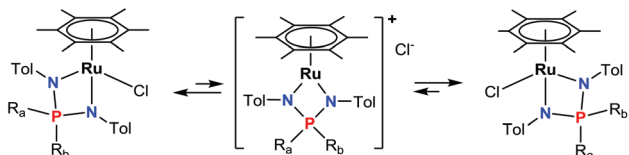


Fig. 7 VT NMR spectra of complex **3b** recorded in CD_2Cl_2 at $T = 193\text{--}298\text{ K}$ (x – stands for grease).



Scheme 2 The exchange between R_a and R_b substituents *via* putative dissociation–association of the chloride anion.⁵³

complex **4c** (δ 80.8). The ^1H NMR spectra of **3c** and **4c** in CDCl_3 are nearly identical and in line with the cationic C_{2v} -symmetric complex. Hence, in sharp contrast to **3a,b**, in CDCl_3 solution **3c** undergoes facile dissociation to give the cationic complex $[(\eta^6\text{-C}_6\text{Me}_6)\text{Ru}\{\text{Ph}_2\text{P}(\text{NMe})_2\}]^+\text{Cl}^-$, which is prevalent in the equilibrium mixture. Apparently strongly electron-releasing *N*-methyl substituents enhance the π -donating ability of the NPN-ligand compared to that of the complexes **3a,b** bearing weaker *N*-tolyl donors.

The arene ruthenium complexes having monoanionic β -diketiminato³⁹ and dianionic bis(imidazolin-2-iminate)⁴⁸ ligands have also been reported earlier to undergo facile chloride dissociation, whereas in the amidinate ruthenium complexes the counter-ion dissociation has been observed only for the weakly coordinating triflate ligand but not the chloride.⁵¹ Hence the capability of the iminophosphonamide ligand to donate electrons and to stabilize the electron-deficient states is much higher than that of the amidinate ligand and comparable to the β -diketiminato and zwitterionic bis(imidazolin-2-iminate) ligands.

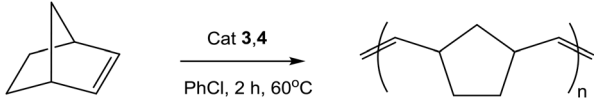
In the UV-vis spectra the complexes **4a–c** have a broad medium intensity band at λ_{max} 540–550 nm shifted to lower energies compared to the corresponding complexes **3a,b** (in CH_2Cl_2) and **3c** (in C_6H_6) having a band at λ_{max} 410–450 nm. Similar bands at λ_{max} 520–530 nm have also been observed for $16\bar{e}$ pentamethylcyclopentadienyl amidinate,²⁹ β -diketiminato⁴⁷ and bis(imidazolin-2-iminate)⁴⁸ ruthenium complexes, which has been attributed to d–d centered transitions.⁴⁷

The $16\bar{e}$ complexes **4a–c** are remarkably stable in solution to air and moisture in sharp contrast to the $18\bar{e}$ complexes **3a–c**, which hydrolyze to produce the corresponding phosphinoides $\text{R}_2\text{P}(\text{O})(\text{NHR}')$. Apparently the nitrogen atoms in **3a–c** are highly basic due to their free electron pairs and thus are prone to the attack by water molecules, whereas in **4a–c** these electron pairs participate in π -bonding to the ruthenium atom and are much less basic. Indeed, the susceptibility to hydrolysis is higher for the complex bearing more electron-releasing *N*-substituents; thus **3c** decomposes within minutes in wet CD_2Cl_2 while **3a,b** are stable for hours. Under similar conditions **4a–c** do not hydrolyze and do not form the $18\bar{e}$ aqua NPN-complexes; their NMR spectra in dried and wet solvents are the same and remain unchanged for days. However, when 10 equivalents of MeCN were added to a solution of **4a** in CD_2Cl_2 the colour immediately changed from violet to red and the phosphorus resonance shifted from δ 72.2 to δ 63.8 indicating the formation of the new complex, presumably the cationic adduct $[(\eta^6\text{-C}_6\text{Me}_6)\text{Ru}(\text{MeCN})\{\text{Ph}_2\text{P}(\text{N-}i\text{-}p\text{-Tol})_2\}](\text{PF}_6)$. The attempt to isolate it by removing the excess of acetonitrile *in vacuo* returned the starting complex **4a** (violet solution in CD_2Cl_2 with the phosphorus resonance at δ 71.0, no acetonitrile signal in ^1H NMR). Bubbling carbon monoxide into a solution of **4a** in CH_2Cl_2 leads to the formation of a yellow CO adduct ($\nu_{\text{CO}} = 1984\text{ cm}^{-1}$), however the CO ligand is labile and easily decoordinates upon removing the solvent under reduced pressure to give back **4a**. A similar $16\bar{e}$ ruthenium iminophosphonamide **5** has also been recently reported to coordinate reversibly CO to form the unstable CO adduct ($\nu_{\text{CO}} = 1993\text{ cm}^{-1}$) and to not react with Cl^- , PPh_3 , and $\text{P}(\text{O}i\text{Pr})_3$.²⁶ In sharp contrast, the more electron-deficient arene ruthenium amidinate $[(\eta^6\text{-C}_6\text{H}_6)\text{Ru}\{\text{PhC}(\text{N}^t\text{Bu})_2\}](\text{BAR}^F_4)$ readily forms the stable carbonyl complex $[(\eta^6\text{-C}_6\text{H}_6)\text{Ru}(\text{CO})\{\text{PhC}(\text{N}^t\text{Bu})_2\}](\text{BAR}^F_4)$, in which the CO band is observed at a much higher frequency ($\nu_{\text{CO}} = 2050\text{ cm}^{-1}$).³⁰ On the other hand, the carbonyl band in the arene ruthenium complex with the dianionic dithiolate ligand $[(\eta^6\text{-C}_6\text{Me}_6)\text{Ru}(\text{CO})(\text{SXyl})_2]$ ($\nu_{\text{CO}} = 1965\text{ cm}^{-1}$)⁵⁴ is close to that in the CO adduct of the iminophosphonamide **4a** and hence indirectly evidences for the zwitterionic nature of the NPN-ligand. Apparently in cationic iminophosphonamides **4a–c** the positive charge is predominantly located on the phosphorus atom rather than on the ruthenium atom and thus their electronic properties are more like those of neutral arene ruthenium complexes with dianionic ligands.

ROMP polymerization of norbornene

Half-sandwich arene ruthenium complexes with sterically bulky phosphanes have been shown earlier to be readily acces-



Table 2 Experimental data for the ring-opening metathesis polymerization of norbornene catalyzed by complexes 3–4^a


Entry	Complex	Monomer conv. (%)	Polymer yield (%)	M_n (kg mol ⁻¹)	M_w/M_n
1	3a	87	76	50	2.7
2	3b	93	82	36	2.5
3	3c	59	51	40	6.9
4	4a	91	70	283	1.65
5	4b	98	79	341	1.55
6	4c	10	6	—	—

^a Norbornene (7.5 mmol); catalyst (0.03 mmol); TMSD (0.1 mmol); chlorobenzene (30 mL); 2 h at 60 °C under argon.

sible precatalysts for ring-opening metathesis polymerization of both strained (norbornene) and low-strain (cyclooctene) cycloolefins and their functionalized derivatives.^{55,56} Typically, the polymers obtained from norbornene had a number-average molecular weight M_n of 60–80 × 10³ and a molecular weight distribution M_w/M_n of 1.6. We have demonstrated that under the same catalytic conditions the complexes 3a–c and 4a,b activated by trimethylsilyldiazomethane (TMSD) catalyze the polymerization of norbornene, except for almost inactive 4c (Table 2).

The 18e complexes 3a–c produced polymers of low molecular weight $M_n = 36–50 \times 10^3$, which is close to the expected $M_n = 23.5 \times 10^3$ calculated from the catalyst/substrate ratio (1/250), meaning that all ruthenium centers are involved in catalysis. The molecular weight distribution is relatively wide: M_w/M_n is 2.5–2.7 for 3a,b and is 6.9 for 3c. The polydispersity of the polymer can be significantly improved when 16e complexes 4a,b are employed. They yield polymers of a much higher molecular weight $M_n = 283–341 \times 10^3$, which is supposedly due to their limited solubility in chlorobenzene and hence only a minor fraction (about 10%) of these cationic complexes can participate in the catalytic cycle. This assumption would mean that the actual activity of 4a,b is about ten times higher than that of 3a,b. Both types of complexes give a considerable fraction (11–20%) of low-weight oligomers soluble in methanol.

In the absence of TMSD the ruthenium iminophosphonamides studied are inactive. The actual catalytically active species in the ROMP of olefins are carbene complexes, which are typically generated *in situ* from the precatalysts and TMSD. Recently, the 16e cationic ruthenium amidinate complexes have been reported to react with TMSD to result in migration of the SiMe₃ group to the ruthenium atom and formation of the amidinato-carbene complexes, in which the carbene moiety is inserted into the RuNCN metallacycle.⁵⁷ These amidinate complexes provided low activity in the ROMP polymerization of norbornene; higher activity was mentioned for polymerization of high-strain norbornadiene catalyzed by the 18e complex [(C₆H₆)RuBr{MeC(NⁱPr)₂}] although the detailed results were not published.³² Perhaps, a similar carbene inser-

tion into the Ru–N bond occurs in the NPN-precatalysts.⁵⁸ Not surprisingly, the more electron rich iminophosphonamide arene ruthenium complexes 3a,b and 4a,b excel the corresponding ruthenium amidinates in the ROMP polymerization of norbornene. However, our attempts to involve them in the ROMP of low-strain cyclooctene were unsuccessful.

It is noteworthy that strongly electron-releasing *N*-methyl substituents drastically decrease the activity of the complexes 3c and 4c. The negligible activity of the 16e complex 4c could be a result of very efficient stabilization of the unsaturated ruthenium center to make it unsusceptible to the reaction with the generated *in situ* carbene CHSiMe₃ rather than of the solubility issues. The same can be attributed to the reduced activity of 3c, which should partially dissociate in polar chlorobenzene to form stable 16e cationic species (*vide supra*).

Experimental

General procedures

All manipulations were carried out using standard Schlenk techniques under an atmosphere of dry argon. Solvents were purified by standard methods and distilled prior to use. Ph₂PCL and Et₂PCL were distilled under high vacuum or at ambient pressure, respectively, prior to use; other commercially available compounds were used as received. ¹H, ³¹P and ¹³C NMR spectra were obtained on a Bruker AMX-400 spectrometer and referenced to the residual signals of deuterated solvent (¹H and ¹³C), and to 85% H₃PO₄ (³¹P, external standard). Elemental analyses were performed on a Carlo Erba 1106 CHN analyzer. The following compounds were prepared according to described procedures: [Ph₂P(NH-*p*-Tol)₂]Br (1a),³⁶ [(η⁶-C₆Me₆)RuCl₂]₂,⁵⁹ Na[B(3,5-C₆H₃(CF₃)₂)₄](NaBAR^F₄).⁶⁰

Synthesis of [Et₂P(NH-*p*-Tol)₂]Br (1b). To a solution of Et₂PCL (2.67 g, 21.5 mmol) in CH₂Cl₂ (30 mL) cooled to 0 °C a solution of Br₂ (1.10 mL, 21.5 mmol) in CH₂Cl₂ (30 mL) was added dropwise. The reaction mixture was warmed to 20 °C, stirred for 1.5 h and cooled again to 0 °C. A solution of *p*-toluidine (9.2 g, 86 mmol) in CH₂Cl₂ (50 mL) was added to the reaction mixture and the resulting suspension was stirred over-



night at 20 °C. The precipitate was filtered off and washed with CH₂Cl₂ (3 × 20 mL). The filtrate was evaporated to dryness and the oily product was stirred with ethyl acetate (150 mL) for 2 h. The fine crystal formed was filtered off, washed with ethyl acetate (3 × 10 mL) and dried *in vacuo* to yield 5.80 g of **1b**. The filtrate was concentrated to 30 mL and left overnight. The precipitated crystal was filtered off, washed with ethyl acetate (3 × 3 mL) and dried *in vacuo* to give additionally 0.92 g of the product. The total yield was 6.72 g (82%). Anal. calcd for C₁₈H₂₆BrN₂P: C, 56.70; H, 6.87; N, 7.35%. Found: C, 56.92; H, 6.96; N, 7.33%. ³¹P NMR (CDCl₃): δ 50.4. ¹H NMR (CDCl₃): δ 8.77 (d, ²J_{HP} = 13.6, 2H, NH), 7.28 (d, ³J = 8.0, 4H, C₆H₄), 6.85 (d, ³J = 8.0, 4H, C₆H₄), 2.62 (dq, ³J_{HP} = 14.0, ³J = 7.6, 4H, CH₂CH₃), 2.15 (s, 6H, Me_{Tol}), 1.04 (dt, ⁴J_{HP} = 21.1, ³J = 7.6, 6H, CH₂CH₃). ¹³C NMR (CDCl₃): δ 135.6 (br. s, i-C_{Tol}(N)), 133.3 (s, i-C_{Tol}(Me)), 130.1 (s, β-C_{Tol}), 119.7 (br. s, α-C_{Tol}), 20.6 (s, Me_{Tol}), 14.7 (d, ¹J_{CP} = 80, CH₂Me), 4.8 (s, CH₂Me).

Synthesis of [Ph₂P(NHMe)₂]Br (1c). To a solution of Ph₂PCL (4.35 mL, 24.0 mmol) in CH₂Cl₂ (50 mL) at room temperature a solution of Br₂ (1.23 mL, 24.0 mmol) in CH₂Cl₂ (15 mL) was added dropwise. The reaction mixture was stirred for 1.5 h and cooled to -50 °C. A freshly prepared cold solution of dimethylamine in CH₂Cl₂ (3 M, 75 mL, 225 mmol) was added to the reaction mixture and the resulting suspension was stirred overnight at 20 °C. The precipitate was filtered off and washed with CH₂Cl₂ (3 × 40 mL). The filtrate was evaporated to dryness and then washed with benzene (5 × 20 mL) and acetone (5 × 20 mL). The white crystalline residue was dried *in vacuo* to yield 6.25 g of **1c** (80%). Anal. calcd for C₁₄H₁₈BrN₂P: C, 51.71; H, 5.58; N, 8.61%. Found: C, 51.89; H, 5.74; N, 8.69%. ³¹P NMR (CDCl₃): δ 40.2. ¹H NMR (CDCl₃): δ 7.97 (dd, ³J_{HP} = 13.0, ³J = 8.2, 4H, *o*-H_{Ph}), 7.51 (dt, ³J = 7.6, ⁵J_{HP} = 1.0, 2H, *p*-H_{Ph}), 7.40 (dt, ³J = 8.0, ⁴J_{HP} = 3.6, 4H, *m*-H_{Ph}), 6.61 (dq, ²J_{HP} = 16.2, ³J = 5.4, 1H, NH), 2.57 (dd, ³J_{HP} = 13.0, ³J = 5.4, 6H, NMe). ¹³C NMR (CDCl₃): δ 123.0 (d, ¹J = 126.0, i-C_{Ph}), 132.4 (d, ²J = 11.2, *o*-C_{Ph}), 129.5 (d, ³J = 13.7, *m*-C_{Ph}), 133.9 (d, ⁴J = 2.7, *p*-C_{Ph}), 26.1 (s, NMe).

Synthesis of [Ph₂P(N-*p*-Tol)(NH-*p*-Tol)] (2a). To a suspension of **1a** (2.00 g, 4.19 mmol) in benzene (50 mL) at room temperature neat Et₂NH (0.45 mL, 4.35 mmol) was added. The mixture was stirred for 4 h. The fine microcrystal was filtered off, washed with benzene (2 × 20 mL) and discarded. The filtrate was evaporated to dryness, and the residue was washed with 10 mL of Et₂O/hexane = 1/2 (v:v). Finally, it was redissolved in benzene; the hazy solution was filtered to remove the traces of the ammonium salts and then evaporated to give off-white powder. Yield 1.62 g (97%). Anal. calcd for C₂₆H₂₅N₂P: C, 78.77; H, 6.36; N, 7.06%. Found: C, 78.94; H, 6.49; N, 6.95%. ³¹P NMR (CDCl₃): δ -3.5. ¹H NMR (CDCl₃): δ 7.93 (ddd, ³J_{HP} = 12.4, ³J = 8.1, ⁴J = 1.8, 4H, *o*-H_{Ph}), 7.39–7.51 (m, 6H, *m,p*-H_{Ph}), 6.96 (d, ³J = 7.5, 4H, C₆H₄), 6.92 (d, ³J = 7.5, 4H, C₆H₄), 5.55 (br. s, 1H, NH), 2.21 (s, 6H, CH₃). ¹³C NMR (C₆D₆): δ 132.7 (d, ¹J = 130.6, i-C_{Ph}), 132.2 (d, ²J = 9.1, *o*-C_{Ph}), 131.3 (s, *p*-C_{Ph}), 129.8 (s, β-C_{Tol}), 128.9 (br. s, i-C_{Tol}(Me)), 128.5 (d, ³J = 12.9, *m*-C_{Ph}), 121.3 (br. d, ³J = 11.8, α-C_{Tol}), 20.5 (s, Me_{Tol}).

Synthesis of [Et₂P(N-*p*-Tol)(NH-*p*-Tol)] (2b). To a solution of **1b** (0.76 g, 2.0 mmol) in benzene (30 mL) at room temperature a 2.0 M solution of NaHMDS (1.0 mL, 2.0 mmol) in THF was added and the mixture was stirred for 2 h. The precipitate of NaBr was filtered off and washed with benzene (3 × 5 mL). The filtrate was evaporated to dryness and the oily residue was washed with hexane (2 × 3 mL) to give quantitatively the product. For an analytical purity the product was recrystallized from warm diethyl ether. Yield 0.55 g (92%). Anal. calcd for C₁₈H₂₅N₂P: C, 71.97; H, 8.39; N, 9.33%. Found: C, 71.95; H, 8.41; N, 9.27%. ³¹P NMR (CDCl₃): δ 23.3. ¹H NMR (CDCl₃): δ 6.96 (br. s, 8H, C₆H₄), 3.85 (br. s, 1H, NH), 2.24 (s, 6H, CH₃), 2.07 (dq, ²J_{HP} = 14.4, ³J = 7.6, 4H, CH₂CH₃), 1.12 (dt, ³J_{HP} = 18.5, ³J = 7.6, 6H, CH₂CH₃). ¹³C NMR (C₆D₆): δ 144.5 (br. s, i-C_{Tol}(N)), 128.6 (s, i-C_{Tol}(Me)), 129.9 (s, β-C_{Tol}), 121.1 (d, ³J_{CP} = 12, α-C_{Tol}), 20.5 (s, Me_{Tol}), 18.9 (d, ¹J_{CP} = 87, CH₂Me), 6.4 (d, ²J_{CP} = 3, CH₂Me).

Synthesis of [Ph₂P(NMe)(NHMe)] (2c). To a suspension of **1c** (1.00 g, 3.05 mmol) in THF (50 mL) at room temperature a 2.0 M solution of NaHMDS (1.5 mL, 3.0 mmol) in THF was added and the mixture was stirred for 18 h. The precipitate of NaBr was filtered off and washed with THF (3 × 5 mL). The filtrate was evaporated to dryness and the oily residue was washed with hexane (2 × 3 mL) and dried *in vacuo* to give a colorless glassy solid. Yield 0.72 g (96%). ³¹P NMR (CDCl₃): δ 12.4. ¹H NMR (THF-*d*₈): δ 7.95 (ddd, ³J_{HP} = 11.2, ³J = 7.6, ⁴J = 2.0, 4H, *o*-H_{Ph}), 7.45–7.52 (m, 6H, *m,p*-H_{Ph}), 2.81 (d, ³J_{HP} = 18.0, 6H, CH₃).

Synthesis of [(η⁶-C₆Me₆)RuCl₂{R₂P(N-*p*-Tol)}₂] (3a,b). General procedure. To a solution of **2a** (0.80 g, 2.02 mmol) in benzene (60 mL) a 2.0 M solution of NaHMDS in THF (1.10 mL, 2.20 mmol) was added and the resulting solution was stirred for 1 h. Then the solid [(η⁶-C₆Me₆)RuCl₂]₂ (0.67 g, 1.00 mmol) was added and the reaction mixture was stirred overnight. The solvent was removed *in vacuo*, the residue was washed with hexane (2 × 10 mL) and extracted with CH₂Cl₂ (100 mL). The filtrate was diluted with 10 mL of benzene and slowly evaporated to 3–5 mL. The precipitated brick-red crystal was filtered off, washed with benzene (2 mL), Et₂O (10 mL) and dried under vacuum. Yield 1.20 g (86%). Anal. calcd for C₃₈H₄₂Cl₂N₂PRu: C, 65.74; H, 6.10%. Found: C, 65.87; H, 6.29%. ³¹P NMR (CDCl₃): δ 43.9. ¹H NMR (CDCl₃): δ 7.76 (br. dd, ³J_{HP} = 12, ³J = 8, 4H, *o*-H_{Ph}), 7.44 (br. t, 2H, *p*-H_{Ph}), 7.33 (br. m, 4H, *m*-H_{Ph}), 6.88 (d, ³J = 8.0, 4H, C₆H₄), 6.78 (d, ³J = 8.0, 4H, C₆H₄), 2.10 (s, 6H, Me_{Tol}), 1.95 (s, 18H, C₆Me₆). ¹H NMR (C₆D₆): δ 8.07 (m, 2H, *o*-H_{Ph}), 7.91 (ddd, ³J_{HP} = 11.2, ³J = 8.0, ³J = 1.6, 2H, *o'*-H_{Ph}), 7.35 (dd, ³J = 8.0, ⁴J_{HP} = 1.2, 4H, C₆H₄), 7.23 (m, 3H, (*p'* + *m*)-H_{Ph}), 6.89 (d, ³J = 8.0, 4H, C₆H₄), 6.73 (m, 3H, (*p* + *m'*)-H_{Ph}), 2.10 (s, 6H, Me_{Tol}), 1.80 (s, 18H, C₆Me₆). ¹³C NMR (CDCl₃): δ 144.6 (d, ²J_{CP} = 4.4, i-C_{Tol}(N)), 133.2 (d, ²J_{CP} = 10.9, *o*-C_{Ph}), 131.4 (d, ⁴J_{CP} = 2.0, *p*-C_{Ph}), 128.5 (s, β-C_{Tol}), 127.9 (s, i-C_{Tol}(Me)), 127.6 (d, ³J_{CP} = 12.7, *m*-C_{Ph}), 125.1 (d, ³J = 9.3, α-C_{Tol}), 89.2 (s, C₆Me₆), 20.5 (s, Me_{Tol}), 16.2 (s, C₆Me₆). UV-vis (CH₂Cl₂; λ_{max}, nm; ε, M⁻¹ cm⁻¹): 450 (900).

Analogously, from **2b** (0.51 g, 1.70 mmol) in THF (50 mL), NaHMDS (2.0 M, 0.90 mL, 1.80 mmol) and [(η⁶-C₆Me₆)RuCl₂]₂



(0.56 g, 0.85 mmol), complex **3b** was obtained. The product was purified by precipitation from a benzene solution (3–5 mL) with hexane (10–15 mL) and further recrystallized from Et₂O. Yield 0.74 g (73%). Anal. calcd for C₃₀H₄₂ClN₂PRu: C, 60.24; H, 7.08%. Found: C, 60.37; H, 7.11%. ³¹P NMR (CDCl₃): δ 72.4. ¹H NMR (CDCl₃): δ 7.04 (d, ³J = 8.0, 4H, C₆H₄), 6.89 (d, ³J = 8.0, 4H, C₆H₄), 2.23 (s, 6H, Me_{Tol}), 1.89 (s, 18H, C₆Me₆), 1.77 (dq, ²J_{HP} = 11.7, ³J = 7.6, 4H, CH₂CH₃), 1.05 (dt, ³J_{HP} = 16.2, ³J = 7.6, 6H, CH₂CH₃). ¹H NMR (C₆D₆): δ 7.48 (d, ³J = 7.7, 4H, C₆H₄), 7.11 (d, ³J = 7.7, 4H, C₆H₄), 2.33 (s, 6H, Me_{Tol}), 2.17 (br. dq, ²J_{HP} = 14.4, ³J = 7.8, 2H, CH₂CH₃), 1.86 (s, 18H, C₆Me₆), 1.47 (br. dt, ³J_{HP} = 15.6, ³J = 7.2, 3H, CH₂CH₃), 1.31 (br. dq, ²J_{HP} = 14.4, ³J = 7.2, 2H, CH₂CH₃), 0.54 (br. dt, ³J_{HP} = 15.6, ³J = 7.8, 3H, CH₂CH₃). ¹³C NMR (CDCl₃): δ 145.1 (d, ²J_{CP} = 4.0, i-C_{Tol}(N)), 128.9 (s, i-C_{Tol}(Me)), 128.8 (s, β-C_{Tol}), 126.1 (d, ³J_{CP} = 6.7, α-C_{Tol}), 88.7 (s, C₆Me₆), 25.7 (d, ¹J_{CP} = 54.8, CH₂Me), 20.6 (s, Me_{Tol}), 15.9 (s, C₆Me₆), 6.5 (d, ²J_{CP} = 4.8, CH₂Me). UV-vis (CH₂Cl₂; λ_{max}, nm; ε, M⁻¹ cm⁻¹): 450 (940).

Synthesis of [(η⁶-C₆Me₆)RuCl{Ph₂P(NMe)₂}] (3c). To a solution of **1c** (0.76 g, 2.3 mmol) in THF (50 mL) a 2.0 M solution of NaHMDS in THF (1.20 mL, 2.40 mmol) was added and the resulting solution was stirred for 3 h. The precipitate of NaBr was removed by filtration, the filtrate was treated again with a 2.0 M solution of NaHMDS (1.2 mL, 2.4 mmol) and stirred for an extra 3 h. Then the solid [(η⁶-C₆Me₆)RuCl₂]₂ (0.77 g, 1.15 mmol) was added and the reaction mixture was stirred overnight. The solvent was removed *in vacuo*, and the residue was washed with hexane (2 × 10 mL) and extracted with benzene (40 mL). The filtrate was diluted with 40 mL of hexane, and the flocculated black impurities were filtered off. The solution was evaporated to 5–7 mL and set for crystallization in a fridge at –20 °C. The precipitated dark-red crystalline was filtered off, washed with cold hexane (5 mL) and dried under vacuum. Yield 0.77 g (62%). Anal. calcd for C₂₆H₃₄ClN₂PRu: C, 57.61; H, 6.32%. Found: C, 57.40; H, 6.38%. ³¹P NMR (C₆D₆): δ 59.8. ³¹P NMR (CDCl₃): δ 76.9. ¹H NMR (C₆D₆): δ 8.00 (br. s, 2H, *o*-H_{Ph}), 7.69 (br. s, 2H, *o*-H_{Ph}), 7.21 (br. s, 3H, (*m* + *p*)-H_{Ph}), 7.12 (br. s, 1H, *p*'-H_{Ph}), 7.05 (br. s, 2H, *m*'-H_{Ph}), 2.74 (d, ³J_{HP} = 19.2, 6H, NMe), 1.84 (s, 18H, C₆Me₆). ¹H NMR (CDCl₃): δ 7.55 (td, ³J = 7.2, ⁵J_{HP} = 1.2, 2H, *p*-H_{Ph}), 7.44 (td, ³J = 8.0, ⁴J_{HP} = 2.8, 4H, *m*-H_{Ph}), 7.26 (dd, ³J_{HP} = 10.4, ³J = 8.0, 4H, *o*-H_{Ph}), 2.71 (d, ³J_{HP} = 19.2, 6H, NMe), 2.27 (s, 18H, C₆Me₆). ¹³C NMR (C₆D₆): δ 140.6 (d, ¹J_{CP} = 104.0, i-C_{Ph}), 132.2 (d, ¹J_{CP} = 58.2, i-C_{Ph}'), 134.9 (br. s., *o*-C_{Ph}), 131.3 (br. s., *p*-C_{Ph}), 130.5 (br. s., (*m* + *m*')-C_{Ph}), 130.2 (br. s., (*o*' + *p*')-C_{Ph}), 88.7 (s, C₆Me₆), 32.9 (s, NMe), 15.6 (s, C₆Me₆). UV-vis (toluene; λ_{max}, nm; ε, M⁻¹ cm⁻¹): 410 (1550).

Synthesis of [(η⁶-C₆Me₆)Ru{R₂P(N-*p*-Tol)₂}] (X) (4a, X = PF₆; 4b, X = BF₄; 4c, X = BAR^F₄). **General procedure.** (a) To a solution of **3a** (0.46 g, 0.66 mmol) in CH₂Cl₂ (30 mL), solid AgPF₆ (0.18 g, 0.72 mmol) was added, the color immediately changed from red to deep violet. The reaction mixture was stirred for 3 h and then filtered through a plug of Celite. The solution was concentrated to 2 mL, further addition of Et₂O (10 mL) resulted in the precipitation of a product, which was filtered off, washed with Et₂O (2 × 5 mL) and dried under vacuum.

Yield of **4a** 0.51 g (96%). Anal. calcd for C₃₈H₄₂F₆N₂P₂Ru: C, 56.78; H, 5.27%. Found: C, 56.69; H, 5.12%. ³¹P NMR (CDCl₃): 71.9, –144.4 (sept, *J*_{PF} = 707, PF₆⁻). ¹H NMR (CDCl₃): δ 7.64 (td, ³J = 7.6, ⁵J_{HP} = 1.2, 2H, *p*-H_{Ph}), 7.49 (td, ³J = 7.6, ⁴J_{HP} = 3.2, 4H, *m*-H_{Ph}), 7.38 (dd, ³J_{HP} = 12.0, ³J = 7.2, 4H, *o*-H_{Ph}), 7.02 (d, ³J = 7.6, 4H, C₆H₄), 6.68 (d, ³J = 7.6, 4H, C₆H₄), 2.28 (s, 6H, Me_{Tol}), 2.08 (s, 18H, C₆Me₆). ¹³C NMR (CD₂Cl₂): δ 141.6 (d, ²J_{CP} = 2, i-C_{Tol}(N)), 135.3 (s, i-C_{Tol}(Me)), 134.2 (d, ⁴J_{CP} = 2.3, *p*-C_{Ph}), 132.0 (d, ²J_{CP} = 10.6, *o*-C_{Ph}), 130.1 (s, β-C_{Tol}), 129.3 (d, ³J_{CP} = 12.4, *m*-C_{Ph}), 126.3 (d, ³J = 6.2, α-C_{Tol}), 126.2 (d, ¹J = 90.5, i-C_{Ph}), 89.9 (s, C₆Me₆), 20.8 (s, Me_{Tol}), 16.5 (s, C₆Me₆). UV-vis (CH₂Cl₂; λ_{max}, nm; ε, M⁻¹ cm⁻¹): 540 (1320).

Analogously, from **3b** (0.45 g, 0.75 mmol) and AgBF₄ (0.15 g, 0.77 mmol), complex **4b** was obtained (0.46 g, 93%). Anal. calcd for C₃₀H₄₂BF₄N₂PRu: C, 55.48; H, 6.52%. Found: C, 55.61; H, 6.44%. ³¹P NMR (CDCl₃): δ 102.3. ¹H NMR (CDCl₃): δ 7.14 (d, ³J = 6.0, 4H, C₆H₄), 6.91 (d, ³J = 6.0, 4H, C₆H₄), 2.31 (s, 6H, Me_{Tol}), 2.02 (s, 18H, C₆Me₆), 1.59 (br. dq, ²J_{HP} = 10, ³J = 8, 4H, CH₂CH₃), 0.99 (br. dt, ³J_{HP} = 16, ³J = 8, 6H, CH₂CH₃). ¹³C NMR (CDCl₃): δ 141.4 (d, ²J_{CP} = 4.0, i-C_{Tol}(N)), 134.9 (d, ⁵J_{CP} = 2.0, i-C_{Tol}(Me)), 130.3 (s, β-C_{Tol}), 125.7 (d, ³J_{CP} = 5.2, α-C_{Tol}), 89.2 (s, C₆Me₆), 20.6 (s, Me_{Tol}), 19.8 (d, ¹J_{CP} = 53.6, CH₂Me), 16.3 (s, C₆Me₆), 5.2 (d, ²J_{CP} = 5.4, CH₂Me). UV-vis (CH₂Cl₂; λ_{max}, nm; ε, M⁻¹ cm⁻¹): 540 (1410).

Analogously, from **3c** (0.14 g, 0.26 mmol) and NaBAR^F₄ (0.23 g, 0.27 mmol), complex **4c** was obtained (0.34 g, 96%). Anal. calcd for C₅₈H₄₆BF₄N₂PRu: C, 50.86; H, 3.38%. Found: C, 50.85; H, 3.34%. ³¹P NMR (CDCl₃): δ 80.8. ¹H NMR (CDCl₃): δ 7.71 (br. s., 8H, *o*-H_{BARF}), 7.60 (ttd, ³J = 7.5, ⁴J = 1.5, ⁵J_{HP} = 1.4, 2H, *p*-H_{Ph}), 7.50 (br. s., 4H, *p*-H_{BARF}), 7.46 (td, ³J = 7.5, ⁴J_{HP} = 3.0, 4H, *m*-H_{Ph}), 7.25 (dd, ³J_{HP} = 12.9, ³J = 7.2, 4H, *o*-H_{Ph}), 2.74 (d, ³J_{HP} = 18.3, 6H, NMe), 2.27 (s, 18H, C₆Me₆). ¹³C NMR (CDCl₃): δ 161.7 (q, ¹J_{CB} = 49.8, i-C_B(BAR^F)), 128.7 (qq, ²J_{CF} = 31.2, ³J_{CB} = 2.4, *m*-C(BAR^F)), 117.4 (m, *o*-C(BAR^F)), 134.7 (br. s, *p*-C(BAR^F)), 124.5 (q, ¹J_{CF} = 272.6, CF₃), 133.8 (d, ⁴J_{CP} = 2.4, *p*-C_{Ph}), 131.1 (d, ²J_{CP} = 9.9, *o*-C_{Ph}), 129.3 (d, ³J_{CP} = 11.6, *m*-C_{Ph}), 124.9 (d, ¹J = 87.5, i-C_{Ph}), 89.3 (s, C₆Me₆), 33.2 (s, NMe), 16.4 (s, C₆Me₆). UV-vis (CH₂Cl₂; λ_{max}, nm; ε, M⁻¹ cm⁻¹): 550 (1300).

Typical procedure for the ROMP of norbornene

A 50 mL round-bottom flask equipped with a magnetic stirring bar and capped with a three-way stopcock was charged with the ruthenium complexes **3–4** (0.03 mmol) and degassed chlorobenzene (20 mL) was added under an argon atmosphere. The solution was stirred for a few minutes at room temperature and then in an oil bath thermostated at 60 °C. Norbornene (1.5 M in chlorobenzene, 5 mL, 7.5 mmol) and eventually trimethylsilyldiazomethane, TMSD (0.1 M in a hexanes–chlorobenzene mixture, 1 mL, 0.1 mmol) were added with a syringe, and the reaction mixture was stirred for 2 h at 60 °C. The conversion was monitored by gas chromatography using norbornane as an internal standard. The resulting gel was diluted with CHCl₃ (20 mL) and slowly poured into MeOH (500 mL) under vigorous stirring. The precipitated polymer was filtered, dried under dynamic vacuum, and characterized



Table 3 Crystal data and structure refinement parameters for 3a–c and 4a–c

	3a	3b	3c	4a	4b	4c
Formula	C ₃₈ H ₄₂ ClN ₂ PRu	C ₃₀ H ₄₂ ClN ₂ PRu	C ₂₆ H ₃₄ ClN ₂ PRu	C ₃₈ H ₄₂ F ₆ N ₂ P ₂ Ru	C ₃₀ H ₄₂ BF ₄ N ₂ PRu	C ₅₈ H ₄₆ BF ₂₄ N ₂ PRu
Formula weight	694.22	598.14	542.04	803.74	649.50	1369.82
T, K	100	100	100	100	100	120
Crystal system	Monoclinic	Monoclinic	Triclinic	Monoclinic	Monoclinic	Monoclinic
Space group	P2 ₁ /n	P2 ₁ /c	P $\bar{1}$	P2 ₁ /n	C2/c	P2 ₁ /c
Z/Z'	4/1	4/1	2/1	4/1	8/1	4/1
a, Å	8.6451(9)	9.890(3)	8.8288(13)	9.7804(6)	25.9645(3)	12.2605(8)
b, Å	20.932(2)	36.718(9)	8.8550(13)	32.185(2)	9.96760(10)	28.9349(15)
c, Å	17.7244(19)	8.509(2)	16.886(3)	12.0350(8)	23.1951(3)	17.1266(10)
α , °			87.525(3)			
β , °	99.594(2)	113.639(7)	79.413(2)	107.2960(10)	96.5526(6)	108.197(2)
γ , °			68.626(2)			
V, Å ³	3162.6(6)	2830.4(13)	1208.0(3)	3617.1(4)	5963.76(12)	5771.9(6)
d_{calc} , g cm ⁻³	1.458	1.404	1.490	1.476	1.447	1.576
μ , cm ⁻¹	6.62	7.26	8.42	5.83	6.27	4.18
2 θ_{max} , °	54	60	54	60	60	56
Refls. collected/independent	32 206/6902	26 013/8183	16 106/5286	46 296/10 527	74 134/8695	41 189/13 856
Observed reflections [$I > 2\sigma(I)$]	4730	6453	4315	7940	8146	7865
R ₁	0.0388	0.0385	0.0506	0.0461	0.0218	0.0653
wR ₂	0.0670	0.0835	0.1262	0.1043	0.0641	0.1570
GOF	1.007	1.040	1.036	1.087	1.043	1.060
Residual density, e Å ⁻³ ($d_{\text{max}}/d_{\text{min}}$)	0.798/−0.735	0.761/−0.664	2.120/−0.945	1.526/−0.927	0.568/−0.509	1.277/−0.863

by NMR spectroscopy and GPC in THF using a polystyrene calibration.

X-ray crystal structure determination

Single crystals of **3** and **4** were obtained by slow diffusion of Et₂O to a solution of a complex (**3a**, **4a–c**) in CH₂Cl₂, or by diffusion of hexane to a solution of **3b** and **3c** in benzene. Data collection for all samples was performed on a Bruker SMART APEX II diffractometer (MoK α radiation, $\lambda = 0.71073$ Å) equipped with an Apex II CCD detector. Frames were integrated using the Bruker SAINT software package⁶¹ by a narrow-frame algorithm. A semiempirical absorption correction was applied with the SADABS⁶² program using the intensity data of equivalent reflections. The structures were solved with direct methods and refined by the full-matrix least-squares technique against F^2_{hkl} in anisotropic approximation with the SHELX⁶³ software package. The positions of hydrogen atoms were calculated, and all hydrogen atoms were refined in a riding model with $1.5U_{\text{eq}}(\text{C}_m)$ and $1.2U_{\text{eq}}(\text{C}_i)$, where $U_{\text{eq}}(\text{C}_m)$ and $1.2U_{\text{eq}}(\text{C}_i)$ are respectively the equivalent thermal parameters of the methyl and all other carbon atoms to which the corresponding H atoms are bonded. Detailed crystallographic information is given in Table 3. Crystallographic data have been deposited to the Cambridge Crystallographic Data Centre, CCDC numbers 1475876–1475879, 1494098 and 1494099.

Conclusions

A series of new 18 \bar{e} and 16 \bar{e} hexamethylbenzene ruthenium complexes with the iminophosphonamide ligand have been synthesized and fully characterized. The elongated Ru–Cl bonds and an easy dissociation of the chloride anion in the

18 \bar{e} complexes **3a–c** as well as short Ru–N bonds in the 16 \bar{e} complexes **4a–c** and small puckering of the Ru–N–P–N metallacycle indeed suggest the zwitterionic nature and strong σ, π -donor character of the iminophosphonamide ligand being able to donate 4 \bar{e} or 6 \bar{e} . Due to charge separation between the phosphorus and the nitrogen atoms, the electronic properties of the NPN-ligand are similar to those of dianionic ligands and therefore it can efficiently stabilize 16 \bar{e} electron deficient complexes. Among other arene ruthenium complexes with κ^2 -N,N chelating ligands, the properties of 16 \bar{e} iminophosphonamide complexes resemble those of strongly donating monoanionic β -diketiminates and dianionic bis(imidazolin-2-iminates), and render them air stable unlike the analogous air-sensitive 16 \bar{e} amidinate complexes. Thus arene ruthenium complexes **3a,b** and **4a,b** bearing the strongly donating NPN-ligand perform better than the analogous ruthenium amidinates in the ROMP of strained norbornene. To properly address the unusually low activity of complexes **3c**, **4c** with the most electron-rich NPN-ligand, which seems to block the activation of the ruthenium center by carbene, a deeper mechanistic investigation is required. The detailed kinetic and thermodynamic studies on the dissociation of the chlorides **3a–c** and the coordination of various ligands to their 16 \bar{e} counterparts **4a–c** as well as the ROMP mechanistic study and application in the transfer hydrogenation of ketones are in progress and to be reported soon.

Acknowledgements

The authors thank the Russian Foundation for Basic Research (grant no. 14-03-00345) for financial support.



Notes and references

- R. Vollmerhaus, R. Tomaszewski, P. Shao, N. J. Taylor, K. J. Wiacek, S. P. Lewis, A. Al-Humydi and S. Collins, *Organometallics*, 2005, **24**, 494–507.
- R. Vollmerhaus, P. Shao, N. J. Taylor and S. Collins, *Organometallics*, 1999, **18**, 2731–2733.
- M. Witt, M. Noltemeyer, H.-G. Schmidt, T. Lübber and H. W. Roesky, *J. Organomet. Chem.*, 1999, **591**, 138–147.
- E. Müller, J. Müller, F. Olbrich, W. Brüser, W. Knapp, D. Abeln and F. T. Edelmann, *Eur. J. Inorg. Chem.*, 1998, **1998**, 87–91.
- C. Qi and S. Zhang, *Appl. Organomet. Chem.*, 2006, **20**, 70–73.
- R. Tomaszewski, R. Vollmerhaus, A. Al-Humydi, Q. Wang, N. J. Taylor and S. Collins, *Can. J. Chem.*, 2006, **84**, 214–224.
- K. Albahily, V. Fomitcheva, S. Gambarotta, I. Korobkov, M. Murugesu and S. I. Gorelsky, *J. Am. Chem. Soc.*, 2011, **133**, 6380–6387.
- K. Albahily, V. Fomitcheva, Y. Shaikh, E. Sebastiao, S. I. Gorelsky, S. Gambarotta, I. Korobkov and R. Duchateau, *Organometallics*, 2011, **30**, 4201–4210.
- K. Albahily, S. Licciulli, S. Gambarotta, I. Korobkov, R. Chevalier, K. Schuhen and R. Duchateau, *Organometallics*, 2011, **30**, 3346–3352.
- K. Albahily, Y. Shaikh, E. Sebastiao, S. Gambarotta, I. Korobkov and S. I. Gorelsky, *J. Am. Chem. Soc.*, 2011, **133**, 6388–6395.
- R. Boese, M. Düppmann, W. Kuchen and W. Peters, *Z. Anorg. Allg. Chem.*, 1998, **624**, 837–845.
- R. Schubbe, K. Angermund, G. Fink and R. Goddard, *Macromol. Chem. Phys.*, 1995, **196**, 467–478.
- W.-J. Guo and Z.-X. Wang, *J. Org. Chem.*, 2013, **78**, 1054–1061.
- B. Prashanth and S. Singh, *J. Chem. Sci.*, 2015, **127**, 315–325.
- R. L. Stapleton, J. Chai, N. J. Taylor and S. Collins, *Organometallics*, 2006, **25**, 2514–2524.
- I. V. Shishkov, F. Rominger and P. Hofmann, *Organometallics*, 2009, **28**, 1049–1059.
- B. F. Straub, F. Eisentrager and P. Hofmann, *Chem. Commun.*, 1999, 2507–2508.
- P. Hofmann, I. V. Shishkov and F. Rominger, *Inorg. Chem.*, 2008, **47**, 11755–11762.
- B. F. Straub, F. Rominger and P. Hofmann, *Organometallics*, 2000, **19**, 4305–4309.
- B. F. Straub, F. Rominger and P. Hofmann, *Chem. Commun.*, 2000, 1611–1612.
- B. F. Straub, I. Gruber, F. Rominger and P. Hofmann, *J. Organomet. Chem.*, 2003, **684**, 124–143.
- N. Nebra, C. Lescot, P. Dauban, S. Mallet-Ladeira, B. Martin-Vaca and D. Bourissou, *Eur. J. Org. Chem.*, 2013, 984–990.
- B. F. Straub and P. Hofmann, *Angew. Chem., Int. Ed.*, 2001, **40**, 1288–1290.
- W. Keim, R. Appel, A. Storeck, C. Krüger and R. Goddard, *Angew. Chem., Int. Ed.*, 1981, **20**, 116–117.
- S. Collins, *Coord. Chem. Rev.*, 2011, **255**, 118–138.
- P. J. Bailey, K. J. Grant and S. Parsons, *Organometallics*, 1998, **17**, 551–555.
- T. A. Peganova, A. V. Valyaeva, A. M. Kalsin, P. V. Petrovskii, A. O. Borissova, K. A. Lyssenko and N. A. Ustynyuk, *Organometallics*, 2009, **28**, 3021–3028.
- More correctly, Chart 1 shows the symmetry adapted linear combinations (SALC) of the atomic orbitals. The corresponding molecular orbitals retain the same symmetry elements, however their designation transforms either to A_2 and B_1 or A'' and A' , respectively for the planar or lateral coordination of the metal atom. Here we used the point group symmetries for SALC to be independent of the symmetry of the resulting complex.
- H. Kondo, T. Sue, A. Kageyama, Y. Yamaguchi, Y. Sunada and H. Nagashima, *J. Organomet. Chem.*, 2009, **694**, 795–800.
- T. Hayashida, Y. Yamaguchi, K. Kirchner and H. Nagashima, *Chem. Lett.*, 2001, 954–955.
- Y. Yamaguchi and H. Nagashima, *Organometallics*, 2000, **19**, 725–727.
- H. Nagashima, H. Kondo, T. Hayashida, Y. Yamaguchi, M. Gondo, S. Masuda, K. Miyazaki, K. Matsubara and K. Kirchner, *Coord. Chem. Rev.*, 2003, **245**, 177–190.
- H. Kondo, Y. Yamaguchi and H. Nagashima, *J. Am. Chem. Soc.*, 2001, **123**, 500–501.
- C. Bibal, M. Pink, Y. D. Smurnyy, J. Tomaszewski and K. G. Caulton, *J. Am. Chem. Soc.*, 2004, **126**, 2312–2313.
- C. Bibal, Y. D. Smurnyy, M. Pink and K. G. Caulton, *J. Am. Chem. Soc.*, 2005, **127**, 8944–8945.
- O. V. Gusev, T. A. Peganova, A. V. Gonchar, P. V. Petrovskii, K. A. Lyssenko and N. A. Ustynyuk, *Phosphorus, Sulfur Silicon Relat. Elem.*, 2009, **184**, 322–331.
- O. J. Scherer and P. Klusmann, *Z. Anorg. Allg. Chem.*, 1969, **370**, 171.
- M. Düppmann, W. Kuchen, W. Peters and W. Phosphorus, *Sulfur Silicon Relat. Elem.*, 1997, **129**, 53–58.
- A. D. Phillips, G. Laurenczy, R. Scopelliti and P. J. Dyson, *Organometallics*, 2007, **26**, 1120–1122.
- T. Singh, R. Kishan, M. Nethaji and N. Thirupathi, *Inorg. Chem.*, 2012, **51**, 157–169.
- T. Hayashida and H. Nagashima, *Organometallics*, 2002, **21**, 3884–3888.
- P. J. Bailey, L. A. Mitchell and S. Parsons, *J. Chem. Soc., Dalton Trans.*, 1996, 2839–2841.
- W. W. Seidel, W. Dachtler and T. Pape, *Z. Anorg. Allg. Chem.*, 2012, **638**, 116–121.
- I. J. Munslow, A. R. Wade, R. J. Deeth and P. Scott, *Chem. Commun.*, 2004, 2596–2597.
- C. F. Barboza da Silva, S. Schwarz, M. Galceran Mestres, S. Teijelo López and J. Strähle, *Z. Anorg. Allg. Chem.*, 2004, **630**, 1919–1923.
- A. D. Phillips, O. Zava, R. Scopelliti, A. A. Nazarov and P. J. Dyson, *Organometallics*, 2010, **29**, 417–427.
- A. D. Phillips, K. Thommes, R. Scopelliti, C. Gandolfi, M. Albrecht, K. Severin, D. F. Schreiber and P. J. Dyson, *Organometallics*, 2011, **30**, 6119–6132.



- 48 T. Glöge, D. Petrovic, C. Hrib, P. G. Jones and M. Tamm, *Eur. J. Inorg. Chem.*, 2009, 4538–4546.
- 49 A. Bondi, *J. Phys. Chem.*, 1964, **68**, 441–451.
- 50 R. S. Rowland and R. Taylor, *J. Phys. Chem.*, 1996, **100**, 7384–7391.
- 51 T. Hayashida, H. Kondo, J. I. Terasawa, K. Kirchner, Y. Sunada and H. Nagashima, *J. Organomet. Chem.*, 2007, **692**, 382–394.
- 52 A. D. Bain, *Prog. Nucl. Magn. Reson. Spectrosc.*, 2003, **43**, 63–103.
- 53 Although we observe the formation of the cationic $16\bar{e}$ species in the solution of **3c** in chloroform or dichloromethane proving them to be possible intermediates, the actual exchange mechanism in apolar solvents can be more complicated or even different from the one given in the simplified Scheme 2.
- 54 K. Mashima, H. Kaneyoshi, S. Kaneko, A. Mikami, K. Tani and A. Nakamura, *Organometallics*, 1997, **16**, 1016–1025.
- 55 A. W. Stumpf, E. Saive, A. Demonceau and A. F. Noels, *J. Chem. Soc., Chem. Commun.*, 1995, 1127–1128.
- 56 A. Demonceau, A. W. Stumpf, E. Saive and A. F. Noels, *Macromolecules*, 1997, **30**, 3127–3136.
- 57 T. Hayashida and H. Nagashima, *Organometallics*, 2001, **20**, 4996–4998.
- 58 The model reaction of **4b** with 3 equiv. of TMSD in dichloromethane resulted in a complex mixture of products, one of each having the signal in ^{31}P NMR at δ 78.3 perhaps corresponds to a carbene complex (a characteristic doublet in ^1H NMR at δ 9.2 with $J_{\text{H-P}} = 16$ Hz). To define the structures of all the species formed and their evolution with time in the ROMP catalytic cycle further mechanistic investigation is to be carried out.
- 59 M. Bennett, T. N. Huang, T. Matheson, A. Smith, S. Ittel and W. Nickerson, *Inorg. Synth.*, 1982, **21**, 74–78.
- 60 N. A. Yakelis and R. G. Bergman, *Organometallics*, 2005, **24**, 3579–3581.
- 61 Bruker, *SAINT v7.23A*, 2005.
- 62 G. M. Sheldrick, *SADABS v2008/1*, Bruker/Siemens Area Detector Absorption Correction Program, 2008.
- 63 G. M. Sheldrick, *Acta Crystallogr., Sect. C: Cryst. Struct. Commun.*, 2015, **71**, 3–8.

